Arabidopsis proline-rich protein important for development and abiotic stress tolerance is involved in microRNA biogenesis

Xiangqiang Zhan[a,1], Bangshing Wang[b,1], Hongjiang Li[c], Renyi Liu[c], Rajwant K. Kalia[d], Jian-Kang Zhu[a,b,2], and Viswanathan Chinnusamy[e,2]

[a]Shanghai Center for Plant Stress Biology and Shanghai Institute of Plant Physiology and Ecology, Shanghai Institutes of Biological Sciences, Chinese Academy of Sciences, Shanghai 200032, China; [b]Department of Horticulture and Landscape Architecture, Purdue University, West Lafayette, IN 47907; [c]Department of Botany and Plant Sciences, University of California, Riverside, CA 92521; [d]Central Arid Zone Research Institute, Jodhpur 342003, India; and [e]Division of Plant Physiology, Indian Agricultural Research Institute, New Delhi 110012, India

Contributed by Jian-Kang Zhu, September 19, 2012 (sent for review August 16, 2012)

MicroRNAs (miRNAs) are important for plant development and stress responses. However, factors regulating miRNA metabolism are not completely understood. SICKLE (SIC), a proline-rich protein critical for development and abiotic stress tolerance of *Arabidopsis*, was identified in this study. Loss-of-function *sic-1* mutant plants exhibited a serrated, sickle-like leaf margin, reduced height, delayed flowering, and abnormal inflorescence phyllotaxy, which are common characteristics of mutants involved in miRNA biogenesis. The *sic-1* mutant plants accumulated lower levels of a subset of miRNAs and transacting siRNAs but higher levels of corresponding primary miRNAs than the WT. The SIC protein colocalizes with the miRNA biogenesis component HYL1 in distinct subnuclear bodies. *sic-1* mutant plants also accumulated higher levels of introns from hundreds of loci. In addition, *sic-1* mutant plants are hypersensitive to chilling and salt stresses. These results suggest that SIC is a unique factor required for the biogenesis of some miRNAs and degradation of some spliced introns and important for plant development and abiotic stress responses.

cold stress | hydroxyproline-rich glycoprotein | intron decay | mRNA stability

MicroRNAs (miRNAs) are a class of endogenous small RNAs that function in gene regulation by guiding mRNA cleavage and translational repression and are critical for plant development and stress responses (1–9). The core components involved in miRNA biogenesis have been identified in plants. RNA polymerase II transcribes *MIR* genes; a 5′ 7-methyl guanosine cap and a 3′ poly(A) tail are added to produce primary miRNA (pri-miRNA) transcripts, which form imperfect stem-loop secondary structures by Watson–Crick base pairing between self-complementary foldback regions. In the *Arabidopsis* nucleus, the stem-loop structure of the pri-miRNA is processed by the RNase III enzyme DICER-LIKE1 (DCL1) to produce a pre-miRNA, which is further processed to generate a 21-nt-long miRNA/miRNA* duplex. For accurate dicing, DCL1 requires the help of HYPONASTIC LEAVES1 (HYL1, a dsRNA-binding protein) and SERRATE (SE, a C2H2zinc-finger protein) (10). The HUA ENHANCER 1 (HEN1) methyltransferase catalyzes 2′-O-methylation of the ribose sugar in the 3′ termini of miRNA/miRNA* duplexes (11). HASTY (HST), a homolog of mammalian EXPORTIN 5, helps export methylated miRNA/miRNA* duplexes from the nucleus to the cytosol (12). The mature miRNA is incorporated into ARGONAUTE1 (AGO1), forming an RNA-induced silencing complex, which scans for miRNA-complementary mRNAs and directs the cleavage or translational repression of the target mRNAs (1).

miR173 and miRNA390 direct the biogenesis of transacting siRNAs (ta-siRNAs). Noncoding transcripts from TRANS-ACTING siRNA genes (TAS) are cleaved by the miRNA-containing AGO1/AGO7 complex (13, 14). The cleaved transcripts are converted into dsRNA by RDR6, and these dsRNAs are processed by DCL4 to yield ∼21-nt ta-siRNAs. Like miRNAs, ta-siRNAs negatively regulate gene expression posttranscriptionally (15–18).

Nuclear mRNA cap-binding complex proteins, abscisic acid (ABA) Hypersensitive 1 (ABH1)/Cap-Binding Protein 80 (CBP80), and CBP20 also play important roles in pre-mRNA and pri-miRNA processing. *abh1*/*cbp80* and *cbp20* mutant plants are impaired in the processing of pri-miRNA transcripts into mature miRNAs, resulting in reduced miRNAs. A significant level of overlap in intron splicing and pri-miRNA processing was observed among *se*, *abh1*/*cbp80*, and *cbp20* mutants. Among these, *se* showed the broadest defect in miRNA biogenesis (19). ABH1 may recruit capped pri-miRNAs to the DCL1/HYL1/SE processing complex or protect the capped pri-mRNA from RNA decay (8). In addition, a nuclear RNA-binding protein, DAWDLE, also interacts with DCL1 and is involved in the biogenesis of a subset of miRNAs and siRNAs in *Arabidopsis* (20). The *Arabidopsis ERECTA mRNA UNDER-EXPRESSED* (*EMU*) encodes a protein homologous to the yeast HPR1, which is a component of the suppressor of the Transcriptional defect of Hpr1 by Overexpression (THO) messenger ribonucleoprotein complex. *emu* showed altered splicing of serine/arginine-rich protein pre-mRNAs, suggesting that EMU is important for pre-mRNA splicing. Furthermore, *emu* accumulated lower levels of a subset of miRNAs than the WT (21). Impairment in the RNA decay pathway, as occurs in the *ein5* (*ethylene insensitive 5*) mutant, also leads to a defect in small RNA biogenesis. *EIN5* encodes XRN4 (5′→3′ EXORIBONUCLEASE 4), which is involved in the removal of uncapped mRNAs, and thus prevents RDR (RNA dependent RNA polymerase)-dependent small RNA biogenesis from uncapped mRNAs (22).

Among the core components of miRNA biogenesis, null alleles of *DCL1* and *SE* are lethal, whereas null alleles of *HYL1* are fertile. Hypomorphic mutations in core components of the miRNA biogenesis, export, and action machinery result in pleiotrophic developmental defects, such as a serrated leaf margin, change in flowering time, abnormal inflorescence phyllotaxy, and reduced fertility (22–31). These findings demonstrated that miRNAs have critical roles in plant development.

Author contributions: R.L., J.-K.Z., and V.C. designed research; X.Z., B.W., H.L., R.K., and V.C. performed research; B.W., H.L., R.L., J.-K.Z., and V.C. analyzed data; and X.Z., B.W., R.L., J.-K.Z., and V.C. wrote the paper.

The authors declare no conflict of interest.

[1]X.Z. and B.W. contributed equally to this work.

[2]To whom correspondence may be addressed. E-mail: jkzhu@purdue.edu or viswa_iari@hotmail.com.

This article contains supporting information online at www.pnas.org/lookup/suppl/doi:10.1073/pnas.1216199109/-/DCSupplemental.

Here, an *Arabidopsis* mutant named *sickle-1* (*sic-1*) was identified on the basis of its enhanced transcript stability of a *LUC* transgene. *sic-1* mutant plants are hypersensitive to chilling and salt stresses and display developmental defects that are hallmarks of mutants defective in miRNA biogenesis. The *SICKLE* (*SIC*) gene was cloned and functionally characterized, and our results show that SIC is involved in miRNA biogenesis in *Arabidopsis*.

Results

***sic-1* Mutation Enhances Luciferase mRNA Stability.** A stress-inducible, *RD29A* promoter-driven luciferase (*LUC*) reporter (P_{RD29A}:*LUC*)-based genetic screen (32) was used to isolate mutants with enhanced LUC bioluminescence under cold stress. Seeds harboring P_{RD29A}:*LUC* transgene (herein after referred to as WT) were mutagenized by ethyl methane sulfonate. The M2 seedlings were screened to obtain putative mutants with enhanced LUC bioluminescence after cold stress (33). One such mutant with high LUC bioluminescence after cold stress at 4 °C for 24 h also displayed sickle-like serrated leaf margins, and hence it was named *sickle* (*sic*) and selected for this study. *sic-1* plants emitted higher LUC bioluminescence than WT after cold (0 °C, 24 h), ABA (100 μM, 3 h), and NaCl (150 mM, 3 h) treatments (Fig. S1 *A* and *B*). A time-course analysis of LUC bioluminescence after cold stress showed higher emissions in *sic-1* than in WT plants (Fig. S1*C*). To determine whether the higher bioluminescence in *sic-1* mutant was due to altered expression of the P_{RD29A}: *LUC* reporter, expression level of the highly unstable *LUC* transcript was determined (33, 34). *LUC* transcript was undetectable in WT (Fig. S1*D*), but a high level of *LUC* transcript was detected in *sic-1* after cold stress (Fig. S1*D*). In contrast to the high levels of LUC bioluminescence (Fig. S1*A*) and *LUC* transcript (Fig. S1*D*) in *sic-1*, the endogenous *RD29A* expression was slightly lower in *sic-1* than in WT plants (Fig. S1*E*). *COLD-REGULATED* 15A (*COR15A*) is highly induced by cold stress and is used as common marker gene to study cold-responsive gene expression in addition to *RD29A*. Hence, we examined whether *sic-1* mutation impaired the expression of *COR15A*. *COR15A* expression was slightly higher in *sic-1* than in WT plants (Fig. S1*E*). This indicates that the cold-stress signaling pathway that mediates *COR15A* expression is slightly perturbed by the *sic-1* mutation.

A nuclear run-on assay was performed to examine whether the differences in *LUC* transcript levels were due to differences in the rate of transcription. The result suggests that, in contrast to the several-fold differences in LUC bioluminescence between WT and *sic-1*, their transcription rates of the *LUC* transgene were similar (Fig. S2 *A* and *B*).

Northern analysis showed that a full-length *LUC* transcript was detectable in *sic-1* (Fig. S2*C*), whereas only degradation products were detected in WT (Fig. S2*C*). To confirm that the degradation products observed in WT were *LUC* specific and to determine the cleaved region of the *LUC* transcript, three different regions of *LUC* transcript were used as probe to perform Northern analysis. The results show that both full-length and cleaved transcripts accumulated in *sic-1*, whereas mainly degradation products of *LUC* transcript accumulated in WT (Fig. S2*D*). Together, the results suggest that the *sic-1* mutation enhances the stability of *LUC* transcript.

***SIC* Encodes a Proline-Rich Protein.** A backcrossed F_2 generation from the *sic-1* mutant displayed a 3:1 segregation between WT and mutant bioluminescence phenotypes, which suggests that *sic-1* is a recessive mutation in a single nuclear gene. The *sic-1* mutation was genetically mapped to a 23.3-kb region on chromosome 4. By sequencing genes within this region, a G-to-A change at the 432nd base downstream of the predicted translation initiation codon of *At4g24500* was identified, which resulted in a change of tryptophan at 143 to a premature stop codon. Therefore, *sic-1* is a loss-of-function mutant and possibly a null allele. To confirm that *At4g24500* is *SIC*, a complementation assay was carried out. Transgenic lines expressing the *At4g24500* gene with its native promoter were generated in *sic-1* mutant background, and their LUC bioluminescence was compared with WT after cold stress. All of the transgenic lines had a WT LUC phenotype (Fig. S3*A*), confirming that *At4g24500* is *SIC*.

A second allele of *sic-1* was obtained from the SALK collection (SALK_054171). Although annotation from The Arabidopsis Information Resource (TAIR) shows that the T-DNA insertion is in the last exon of *SIC*, our analysis revealed that the actual insertion is in the 3′ UTR region of *SIC*. Thus, SALK_054171 is a knockdown allele (*sic-2*) with reduced *SIC* expression (Fig. S3*B*).

SIC is annotated as a hydroxyproline-rich glycoprotein with an unknown function (TAIR 10 release; http://www.arabidopsis.org/). *SIC* is a single-copy gene in the *Arabidopsis* genome.

SIC Is Necessary for Normal Plant Development. The *sic-1* mutant displayed a number of developmental phenotypes (Fig. 1*A*). The *sic-1* mutants showed delayed flowering compared with WT, and this delay was more pronounced under short-day light conditions (Fig. S3 *C* and *D*). At maturity, *sic-1* exhibited dwarfism compared with WT (Fig. S3*E*). However, the *sic-2* allele did not show strong developmental phenotypes compared with *sic-1* (Fig. S3*E*), likely because expression of the *SIC* gene was only reduced in the *sic-2* mutant. Developmental defects observed in *sic-1* are common in mutants impaired in miRNA biogenesis and pre-mRNA processing. For example *dcl1*, *se*, *hyl1*, *abh1*/*cbp80*, *cpb20*, *emu*, and *ein5* all produce leaves with serrated margins (21–25, 27, 29, 31, 35, 36). Abnormal inflorescence phyllotaxy (emergence of flowers from the same internode on the inflorescence) was observed in *se-1*, *hyl1-1*, and *smu1-2* (*suppressors of mec-8 and unc-52 1*) plants (24, 31, 37). The leaf-serration phenotype in *sic-1* was compared with those in *se-1* and *abh1-285* mutants. Rosette and cauline leaves of *sic-1*, *se-1*, and *abh1-285* had deeper serrations compared with WT (Fig. 1*A*). The sickle leaf margin phenotype of *sic-1* mutant was corrected in transgenic lines expressing the WT *SIC* gene (*sic-1*:*SIC-GFP* and *sic-1*:*SIC-FLAG*) (Fig. 1*B*). In addition, *sic-1* plants also exhibited an abnormal inflorescence phyllotaxy phenotype similar to *se-1* and *abh1-285* (Fig. 1*C*). Although *sic-1* plants were shorter than WT, the heights of *se-1* and *abh1-285* plants were similar to WT (Fig. S3*F*). The dwarfism

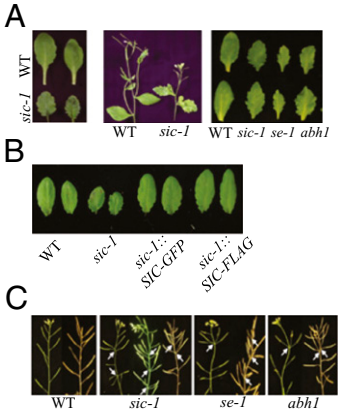

Fig. 1. Effect of *sic-1* on leaf and inflorescence morphology. (*A*) Leaf morphology. Rosette and cauline leaves of *sic-1* have serrated sickle-like margins, in contrast to those of WT. The leaf morphology of *sic-1* is similar to that of *se-1* and *abh1-285*. (*B*) *SIC* rescues the leaf-shape defect of *sic-1*. Rosette leaves of WT, *sic-1*, and *sic-1* genetically transformed with native promoter-driven *SIC* gene (*sic-1*:*SIC-Flag* and *sic-1*:*SIC-GFP*). (*C*) Architecture of silique arrangements in WT, *sic-1*, *se-1*, and *abh1-285*. Arrow shows clustering of more than one silique on the same node in *sic-1*, *se-1*, and *abh1-285*.

and other defects of *sic-1* were corrected in the transgenic lines expressing a WT copy of *SIC* gene (Fig. S3*G*), supporting that SIC is necessary for normal plant development.

SIC Is Involved in miRNA Biogenesis. Because the developmental defects of *sic-1* were similar to those of mutants impaired in miRNA biogenesis, we hypothesized that SIC may function in miRNA biogenesis. Northern analysis revealed that the accumulation of miR159, miR164, miR165, miR166, miR168, miR171, miR172, miR173, miR393, and miR398 was lower in *sic-1* than in WT both in vegetative (seedlings) and reproductive (inflorescence) tissues (Fig. 2*A*). The level of miRNA accumulation was lowest in *se-1* followed by *sic-1* in seedling, whereas in inflorescences many miRNAs were similar in *sic-1* and *se-1* but were lower than in WT. The levels of miRNAs, except for miR164 and miR171, were lower in *sic-1* than in *abh1-285* plants (Fig. 2*A*).

In *Arabidopsis*, *TAS1*, *TAS2*, and *TAS3* genes can give rise to ta-siRNAs. miR173 and miR390 direct the cleavage of *TAS* gene transcripts to initiate ta-siRNA biogenesis (15, 17). Because *sic-1* plants accumulated lower levels of miR173, the expression levels of *TAS1* family of ta-siRNAs, namely ta-siR255, ta-siR752, and ta-siR850, were examined. All three ta-siRNAs accumulated to lower levels in *sic-1* than in WT (Fig. 2*B*). Previous studies have shown that loss-of-function mutations of SE (30), CBP20, and CBP80 (35) lead to reductions in miR173, miR390, and their target ta-siRNAs. Our results provide evidence that ta-siRNA biogenesis also requires SIC. The accumulation level of 24-nt siRNAs was examined to determine whether *sic-1* may affect siRNA levels. Accumulation of 24-nt siRNA at the *AtSN1* locus did not change in *sic-1*, *se-1*, and *abh1-285* compared with WT (Fig. S4*A*). This suggests that SIC is required for biogenesis of DCL1-dependent miRNAs and DCL4-dependent ta-siRNAs, but not for DCL3-dependent repeat-associated siRNAs such as AtSN1.

Previously, *se-1*, *hyl1*, *dcl1*, *abh1-285*, and *cbp20-1* were found to accumulate higher levels of pri-miRNAs but lower levels of mature miRNAs compared with WT (19, 35, 36). Pri-miRNA accumulation in *sic-1* was tested, and the results showed that accumulation of unspliced and spliced pri-miR156a and pri-miRNA164a was higher in *sic-1* than in WT (Fig. 2*C*). Real-time RT-PCR analysis showed that pri-miRNA166a, pri-miRNA166b, and pri-miRNA171b were >twofold more abundant in *sic-1* than in WT (Fig. 2*D*). Although pri-miRNA levels were higher in *sic-1* than in WT, the levels were much lower in *sic-1* than in *se-1* and *abh1-285* (Fig. S4*B*).

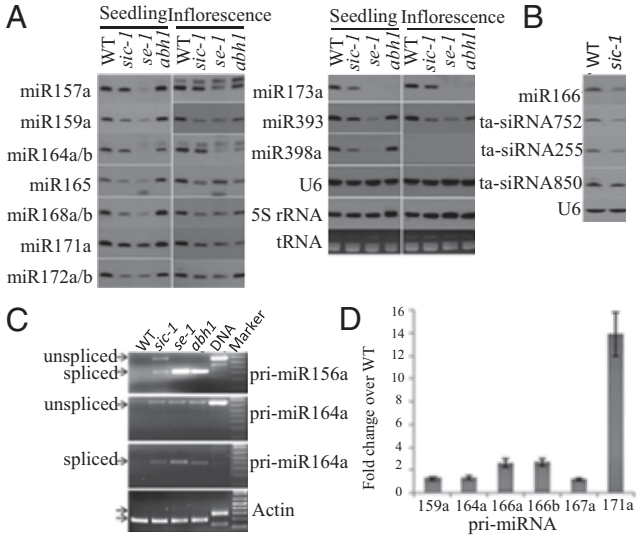

Fig. 2. Effect of *sic-1* on the accumulation of miRNAs, ta-siRNAs, and pri-miRNAs. (*A*) Northern analysis of miRNA accumulation in WT, *sic-1*, *se-1*, and *abh1-285* of *Arabidopsis* seedling and inflorescence. (*B*) Northern analysis of ta-siRNA in WT and *sic-1* in *Arabidopsis*. (*C*) RT-PCR analysis of pri-miRNA accumulation in WT, *sic-1*, *se-1*, and *abh1-285* of *Arabidopsis* (WT, *sic-1*, *se-1*, *abh1* = RT-PCR, DNA = Columbia genomic DNA was used as template for PCR). (*D*) Quantitative RT-PCR analysis of pri-miRNA accumulation in WT and *sic-1* in seedlings.

Expression level of predicted miRNA targets was examined to determine whether the target genes were affected by the *sic-1* mutation. Expression levels of the predicted miR159a, miR166, miR171a, and miR390 target genes (*At1g53230*, *At5g37020*, *At4g00150*, and *At5g14050*, respectively) were higher in *sic-1* than in WT (Fig. S4*C*, *Upper*), which is consistent with the reduced miRNAs in the mutant. On the other hand, the expression levels of predicted miR165, miR172, miR393, and miR397b target genes (*At4g32880*, *At2g39250*, *At1g12820*, and *At2g38080*, respectively) did not change despite reduced miRNA levels (Fig. S4*C*, *Lower*). This is possibly due to multiple target genes and/or that the miRNAs may cause translational inhibition rather than transcript cleavage of the target genes.

To further confirm that the mutation in *SIC* is responsible for the reduction in miRNA levels, miRNA accumulation was examined in the *sic-1* complementation transgenic lines. miR159a and miR398a were restored to WT levels in the transgenic lines (Fig. S4 *D* and *E*). Although miRNA levels in *sic-2* were not as low as in *sic-1*, they were still lower compared with the WT (Fig. S4 *D* and *E*), consistent with *sic-2* being a weaker allele.

Differentially expressed genes were identified in *sic-1* vs. WT by using whole-genome tiling arrays. Among 4,225 differentially expressed genes, 2,135 were up-regulated, and 2,090 were down-regulated in *sic-1* relative to WT (Dataset S1). Five up-regulated and five down-regulated genes were validated by real-time RT-PCR, and the results were consistent with the tiling array data for all 10 genes (Fig. S5 *A* and *B*). Furthermore, tiling array analysis showed that several miRNA target genes were up-regulated in *sic-1* relative to WT (Dataset S2).

***sic-1* Mutation Impairs Intron Decay.** The morphological phenotypes of *sic-1* plants were largely similar to those of *se-1*, *abh1*, *cbp20*, *smu-1*, and *sta1* plants. These latter mutants are impaired in not only miRNA biogenesis but also in pre-mRNA processing. Hence, pre-mRNA processing (intron splicing) was examined by tiling array analysis. We found that *sic-1* mutant plants retained significantly higher levels of introns than the WT (Dataset S3). Thirty-one percent of the accumulated introns were at the first position (Fig. S6). For verification of tiling array data, the top two genes, *CRB* (At1g09340, CHLOROPLAST RNA BINDING) and *CAX1* (At2g38170, a high affinity vacuolar calcium antiporter), which retained higher levels of introns in *sic-1* compared with WT (Dataset S3), were selected for Northern blot analysis. In addition to exon-specific probes, for *CRB* and *CAX1* genes first and second intron-specific probes, respectively, were used. *CAX1* was up-regulated in both WT and *sic-1* in response to cold stress, but *sic-1* accumulated more cleaved introns compared with WT (Fig. 3). Similarly, cleaved introns of *CRB* also accumulated in *sic-1* (Fig. 3). The accumulation of excised introns of *CAX1* and *CRB* were evident in *sic-1* mutant without stress, but the accumulation was increased in response to cold stress (Fig. 3).

SIC Colocalizes with HYL1 in Distinct Subnuclear Bodies. The above results suggest that SIC is localized at the site of RNA processing (i.e., the nucleus). The SIC-GFP fusion exhibited a nuclear localization in root cells (Fig. 4*A*). HYL1 has previously been shown to interact and colocalize with DCL1 in distinct nuclear bodies referred to as "dicing bodies" (38–40). We found that SIC protein was concentrated in distinct nuclear bodies, in addition to diffuse distribution in the nucleoplasm (Fig. 4*B*). Simultaneous immunolocalization of SIC and HYL1 revealed that the two proteins were colocalized in the nuclear bodies (Fig. 4*B*).

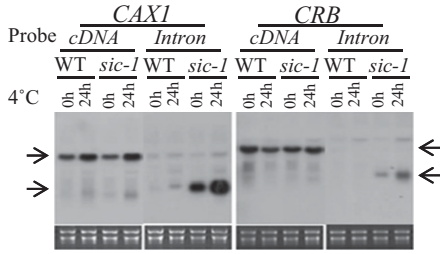

Fig. 3. Effect of *sic-1* on the accumulation of spliced introns. Accumulation of mRNA and spliced intron of *CAX1* (*CATION EXCHANGER 1/RARE COLD INDUCIBLE 4*) and *CRB4* (*CHLOROPLAST RNA BINDING*) genes was determined by Northern analysis.

SIC Is Important for Chilling and Salt Stress Tolerance. In addition to having developmental defects, some mutants involved in miRNA biogenesis and pre-mRNA processing show altered stress responses. For example, *hyl1*, *se*, *abh1*, *cbp20*, *sta1*, and *emu* mutants are hypersensitive to ABA during seed germination (21, 23, 33, 35, 41). *sic-1* was less sensitive to ABA than *se-1* and *abh1-285* during germination and was only slightly more sensitive than WT (Fig. S7 *A* and *B*). Interestingly, *sic-1* was hypersensitive to chilling stress imposed at the germination stage or seedling stage (Fig. 5 *A* and *B*). *sic-1* was more sensitive to chilling stress than *se-1*, *abh1-285*, or WT (Fig. 5*C*). The basal freezing tolerance (before cold acclimation) was higher in *sic-1* than in WT (Fig. S7*C*), but the *sic-1* mutation did not affect acquired freezing tolerance (after acclimation) (Fig. S7*D*). In addition, *sic-1* and *abh1-285* were hypersensitive to 150 mM NaCl, whereas *se-1* was less sensitive than *sic-1* and *abh1-285* (Fig. 5*D*).

Discussion

The *sic-1* mutant was isolated on the basis of enhanced stability of *LUCIFERASE* transgene in *Arabidopsis*. *SIC* (At4g24500) encodes a hydroxyproline-rich protein with unknown biochemical function. *SIC* loss-of-function mutants showed pleiotropic developmental defects including reduction in plant height, delay in flowering, increase in serration at the leaf margin, and abnormal inflorescence phyllotaxy. Mutations in several miRNA biogenesis factors are known to exhibit both serrated leaf margins and abnormal inflorescence phyllotaxy (22–24, 30, 31). Importantly, *sic-1* was deficient in miRNA and ta-siRNA accumulation and accumulated higher levels of unprocessed pri-miRNAs as well as spliced introns from protein-coding genes. miRNA accumulation levels in *sic-1* were lower than in WT but intermediate between *se-1* and *abh1-285*. Like *hyl1* and *hen1* (29, 41), *sic-1* displayed dwarfism, although plant height was not reduced in *se-1* and *abh1-285*. These results suggest that compared with the other miRNA biogenesis factors, SIC performs shared as well as specific roles in miRNA biogenesis and development. The colocalization of SIC with HYL1 in distinct nuclear bodies further supports that SIC is involved in miRNA biogenesis.

Expression analysis confirmed that *sic-1* has lower levels of miRNAs and ta-siRNAs but enhanced accumulation of pri-miRNAs and higher expression of some predicted miRNA target genes. Tiling array analysis showed that *sic-1* plants accumulated high levels of introns for 456 loci. *se-1*, *abh1-285*, and *cbp20* plants showed a significant overlap: 140 loci were commonly affected (19). Like other miRNA biogenesis mutants, *sic-1* accumulated unspliced pri-miRNA, albeit to a lower level than *se-1* and *abh1*, which suggests that SIC is another component involved in miRNA biogenesis. However, in contrast to the other mutants, *sic-1* mutants accumulated spliced introns rather than the unspliced pre-mRNAs. The result suggests that the degradation of some RNAs is slower in *sic-1*. This is consistent with the observation of enhanced stability of *LUC* transcript in *sic-1*.

Reduced biogenesis of miRNAs in the *hyl1* mutant resulted in higher stability of their target transcripts (42). A previous report showed that a mutation in pre-mRNA splicing in *STABILIZED1 (STA1)* gene led to enhanced stability of the *LUC* transcript (33). *sta1* also has serrated leaf margins and defects in mRNA splicing (33). Hence, the enhanced stability of the *LUC* transcript in *sic-1* seems to be due to its defects in RNA metabolism, which includes miRNA and ta-siRNA biogenesis as well as spliced intron decay. These results suggest a possible common mechanism for the cleavage of pri-miRNA hairpins and decay of spliced introns. Although a link between miRNA biogenesis and spliced intron decay was not known before, a connection between nonsense-mediated decay of mRNAs and small RNA biogenesis was previously found in the *ein5-6* mutant of *Arabidopsis*, which is defective in the decay of uncapped mRNAs and showed a marginal reduction in miRNAs but an increase in the 21-nt small RNAs processed from transcripts of proteins coding genes. Defects in miRNA biogenesis and abnormal inflorescence phyllotaxy were further enhanced in the *ein5-6 abh1-1* double mutants (21). Determining the exact mechanisms of action of

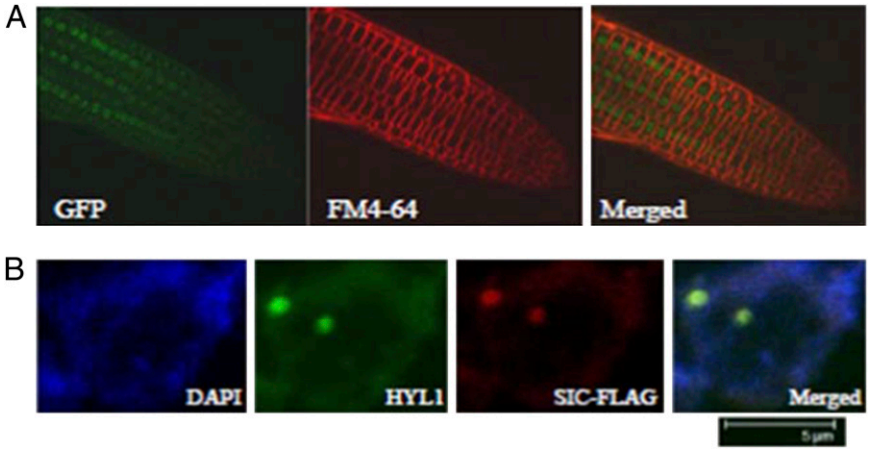

Fig. 4. Colocalization of SIC and HYL1 in distinct nuclear bodies. (*A*) Nuclear localization of the SIC-sGFP. Confocal microscope images of root cells of *SIC-sGFP* transgenic *Arabidopsis* plants. GFP, GFP fluorescence; FM4-64, fluorescence of FM4-64-stained cells; Merged, GFP+FM4-64 superimposed images. (*B*) Colocalization on SIC and HYL1 in distinct nuclear bodies. DAPI, DAPI-stained nuclei; HYL1, immunolocalization of HYL1 with anti-HYL antibody; SIC-FLAG, immunolocalization of SIC-FLAG with anti-FLAG antibody; Merged, merged field images of DAPI, HYL1, and SIC-FLAG.

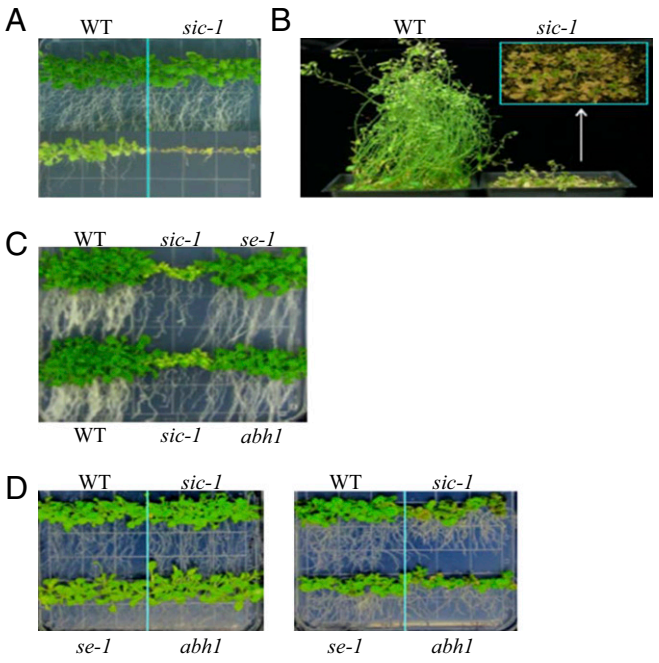

Fig. 5. Abiotic stress responses of the *sic-1* mutant plants. (*A*) Chilling stress response of WT and *sic-1*. Seeds were germinated and grown on MS medium supplemented with 3% sucrose at 22 °C for 3 wk (*Upper*) or at 4 °C for 5 wk (*Lower*). (*B*) WT and *sic-1* seeds were germinated and grown in soil at 22 °C for 3 wk, then transferred to and grown at 4 °C for 2 mo. *Inset*: Top view of the *sic-1* under cold stress. (*C*) Chilling stress response of *sic-1*, *se-1*, and *abh1-285*. (*D*) NaCl stress response of *sic-1*, *se-1*, and *abh1-285*. Six-day-old seedlings were transplanted on to MS medium supplemented with 3% sucrose (*Left*) or with 3% sucrose with 150 mM NaCl (*Right*) and grown for 3 wk.

SIC in miRNA biogenesis, intron splicing, and decay of spliced introns will require further study.

Besides development, miRNAs also regulate abiotic stress responses of plants through posttranscriptional regulation of gene expression (2, 43, 44). The *sic-1* mutation enhanced ABA sensitivity only marginally relative to the *se-1* and *abh1-285* mutations. Interestingly, only *sic-1* showed a dramatic hypersensitivity to chilling. Both *sic-1* and *abh1-285* were more salt sensitive than *se-1* or WT. Although the abundance of stress-regulated miRNAs, such as miR159, miR165, miR168, miR171, miR172, miR393, and miR398 (43, 45, 46), were found to be constitutively low in *sic-1*, *se-1*, and *abh1-285*, only *sic-1* is compromised in chilling tolerance, whereas *se-1* and *abh1-285* were more sensitive to ABA than *sic-1*. This suggests that although SIC, SE, and ABH1 have shared functions in miRNA biogenesis, SE and ABH1 are more important for ABA responses and SIC-dependent RNA metabolism is more important for chilling tolerance in *Arabidopsis*. Therefore, the developmental defects and stress sensitivity of *sic-1* are caused by not only a deficiency in miRNA biogenesis but also other impairments in RNA metabolism.

Postsplicing intron degradation after endonucleolytic cleavage of the excised lariat is not well understood. In yeast, introns in some pre-mRNAs form hairpin structures, which trigger degradation of unspliced pre-mRNAs and lariat introns through RNaseIII (Rnt1p)-mediated cleavage (47). In *Arabidopsis*, a chloroplast polynucleotide phosphorylase (cpPNPase) with an RNase-PH domain is required for degradation of the excised lariat. This cpPNPase also has poly(A) polymerase activity, which may affect stability of poly(A) mRNA, because poly(A) mRNA stability is low in chloroplasts (48). A feature common to the pri-miRNA hairpin and the lariat in the spliced intron is the loop structure. SIC may assist RNase III in the cleavage of the loop to open the lariat. Excised introns can also form a stem-loop structure, which can be processed by small RNA biogenesis machinery to produce miRNAs or siRNAs. Approximately 2% and 7% of small RNAs are derived from the intron hairpins in *Arabidopsis* and rice, respectively (49). We speculate that SIC may bind to the loop structure of the pri-miRNA and lariat, thereby enhancing the cleavage of pri-miRNAs, biogenesis of intron-derived siRNAs, and lariat degradation. It is of interest to test the genetic relationship between SIC and known components involved in miRNA biogenesis, such as SE, ABH1, and DCL1, to understand whether SIC and other known components may work together in the same pathway to regulate miRNA biogenesis.

Materials and Methods

Plant Materials and Mutant Isolation. The Columbia ecotype (with *gl-1* mutation) harboring *RD29A* promoter-driven *LUCIFERASE* reporter gene (here after referred to as WT) was mutagenized with ethyl methanesulfonate. The M_2 seeds were germinated and screened for putative mutants with high LUC bioluminescence under cold stress using a low-light luminescence imaging system with WinView software (Princeton Instruments) (50). One such mutant with high bioluminescence after cold stress at 0 °C for 24 h was designated *sickle-1* (*sic-1*) and was selected for further study.

RNA Analysis. Seedlings were grown on MS agar plates supplemented with 3% sucrose in a growth chamber for 10 d. Cold treated (4 °C) or untreated (24 °C) seedlings were used for total RNA extraction with the RNeasy plant mini kit (Qiagen). Northern analysis and the probes used for *RD29A*, *COR15A*, *LUC*, and *TUBULIN* were described previously (33). For *CAX1* (At2g38170) and *CRB* (At1g09340), the probes from exon and intron region were PCR amplified and confirmed by sequencing.

Accumulation of small RNA was determined by Northern analysis. Total RNA was first extracted from 10-d-old seedlings, rosette leaves, and inflorescence by using TRIzol (Invitrogen). Low-molecular-weight RNA was purified from total RNA, and small RNA Northern analysis was carried out as described previously (51).

Construction of GFP- and FLAG-Tagged Transgenic Plants. A 3,589-bp amplicon consisting of *SIC* with its native promoter (without termination codon and 3′ UTR) was PCR amplified from WT genomic DNA by using Platinum Taq (Invitrogen). This PCR product was cloned into pENTR-D-TOPO (Invitrogen). The donor vector with *SIC* was used for cloning into pEG302 (for FLAG fusion) (52) and pGWB504 (for GFP fusion) (53) by using site-specific recombination with Gateway LR Clonase II enzyme mix (Invitrogen). These constructs were verified by sequencing. The binary construct was then introduced into *Agrobacterium* strain GV3101 and was used for genetic transformation of the *sic-1* plants by the floral dip method. T_1 transformants from *sic-1* plants transformed with pEG302-SIC-FLAG were selected on BASTA-containing MS medium. The pGEB504-SIC-GFP transformants were selected on the basis of hygromycin resistance. These transgenic lines were further confirmed by PCR.

RT-PCR Analysis of Gene Expression. Total RNA (2 μg) was reverse-transcribed using oligo-dT primers and the SuperScript III First-Strand Synthesis System (Invitrogen). A 1-μL quantity of the cDNA was used as a template for all of the downstream applications, such as standard PCR reactions for analysis of pri-miRNAs, and real-time PCR analysis of pri-miRNA accumulation was carried out using iQ SYBR Green Supermix (Bio-Rad). Gene-specific oligonucleotides used in PCR analysis are given in Table S1.

Immunolocalization of FLAG-SIC and HLY1 Proteins. The roots of pGEB504-SIC-GFP transgenic plants were imaged with a Zeiss 510 confocal microscope to localize SIC-GFP fusion protein. SIC and HYL1 localizations were examined by immunostaining as described previously (54). After postfixation, the slides were blocked in KPBS [10× KPBS: 1.28 M NaCl, 20 mM KCl, 80 mM Na_2HPO_4, and 20 mM KH_2PO_4 (pH 7.2)] with 1% BSA and 0.1% Triton X at 37 °C for 30 min. The slides were then washed three times (5 min each time) with KPBS containing 0.1% Triton X. Slides were incubated with mouse monoclonal anti-FLAG antibody (1:400; Sigma-Aldrich) or anti-HYL1 antibody (1:500) overnight at 4 °C. The slides were washed three times with KPBS and then blocked with blocking solution for 30 min at 37 °C in a humid

chamber. The slides were incubated for 2 h at 37 °C in KPBS with 0.1% Triton containing secondary antibody, anti-mouse-FITC (1:100; Sigma) for FLAG-SIC, and goat anti-rabbit-Alexa 594 (1:100; Invitrogen) for HYL1 X. The slides were then washed in KPBS and mounted in antifade reagent with DAPI (Invitrogen). Stained nuclei were observed with a Leica SP2 confocal microscope.

ACKNOWLEDGMENTS. We thank Y. Adam Yuan, Department of Biological Sciences, National University of Singapore, Singapore for providing HYL1 antibody, and Avnish Kapoor for assistance with the nuclear run-on analysis. This work was supported by National Institutes of Health Grants R01GM070795 and R01GM059138 and US Department of Agriculture Grant 2008-35100-04518 (to J.-K.Z) and by the Chinese Academy of Sciences.

1. Jones-Rhoades MW, Bartel DP (2004) Computational identification of plant microRNAs and their targets, including a stress-induced miRNA. *Mol Cell* 14(6):787–799.
2. Sunkar R, Chinnusamy V, Zhu J, Zhu JK (2007) Small RNAs as big players in plant abiotic stress responses and nutrient deprivation. *Trends Plant Sci* 12(7):301–309.
3. Zhu JK (2008) Reconstituting plant miRNA biogenesis. *Proc Natl Acad Sci USA* 105(29): 9851–9852.
4. Voinnet O (2009) Origin, biogenesis, and activity of plant microRNAs. *Cell* 136(4): 669–687.
5. Rubio-Somoza I, Cuperus JT, Weigel D, Carrington JC (2009) Regulation and functional specialization of small RNA-target nodes during plant development. *Curr Opin Plant Biol* 12(5):622–627.
6. Poethig RS (2009) Small RNAs and developmental timing in plants. *Curr Opin Genet Dev* 19(4):374–378.
7. Chuck G, Candela H, Hake S (2009) Big impacts by small RNAs in plant development. *Curr Opin Plant Biol* 12(1):81–86.
8. Chen X (2008) A silencing safeguard: Links between RNA silencing and mRNA processing in *Arabidopsis*. *Dev Cell* 14(6):811–812.
9. Katiyar-Agarwal S, Jin H (2010) Role of small RNAs in host-microbe interactions. *Annu Rev Phytopathol* 48:225–246.
10. Dong Z, Han MH, Fedoroff N (2008) The RNA-binding proteins HYL1 and SE promote accurate in vitro processing of pri-miRNA by DCL1. *Proc Natl Acad Sci USA* 105(29): 9970–9975.
11. Yu B, et al. (2005) Methylation as a crucial step in plant microRNA biogenesis. *Science* 307(5711):932–935.
12. Park MY, Wu G, Gonzalez-Sulser A, Vaucheret H, Poethig RS (2005) Nuclear processing and export of microRNAs in *Arabidopsis*. *Proc Natl Acad Sci USA* 102(10): 3691–3696.
13. Montgomery TA, et al. (2008a) Specificity of ARGONAUTE7-miR390 interaction and dual functionality in TAS3 trans-acting siRNA formation. *Cell* 133(1):128–141.
14. Montgomery TA, et al. (2008b) AGO1-miR173 complex initiates phased siRNA formation in plants. *Proc Natl Acad Sci USA* 105(51):20055–20062.
15. Allen E, Xie Z, Gustafson AM, Carrington JC (2005) microRNA-directed phasing during trans-acting siRNA biogenesis in plants. *Cell* 121(2):207–221.
16. Gasciolli V, Mallory AC, Bartel DP, Vaucheret H (2005) Partially redundant functions of *Arabidopsis* DICER-like enzymes and a role for DCL4 in producing trans-acting siRNAs. *Curr Biol* 15(16):1494–1500.
17. Yoshikawa M, Peragine A, Park MY, Poethig RS (2005) A pathway for the biogenesis of trans-acting siRNAs in *Arabidopsis*. *Genes Dev* 19(18):2164–2175.
18. Xie Z, Allen E, Wilken A, Carrington JC (2005) DICER-LIKE 4 functions in trans-acting small interfering RNA biogenesis and vegetative phase change in *Arabidopsis thaliana*. *Proc Natl Acad Sci USA* 102(36):12984–12989.
19. Laubinger S, et al. (2008) Dual roles of the nuclear cap-binding complex and SERRATE in pre-mRNA splicing and microRNA processing in *Arabidopsis thaliana*. *Proc Natl Acad Sci USA* 105(25):8795–8800.
20. Yu B, et al. (2008) The FHA domain proteins DAWDLE in *Arabidopsis* and SNIP1 in humans act in small RNA biogenesis. *Proc Natl Acad Sci USA* 105(29):10073–10078.
21. Furumizu C, Tsukaya H, Komeda Y (2010) Characterization of EMU, the *Arabidopsis* homolog of the yeast THO complex member HPR1. *RNA* 16(9):1809–1817.
22. Gregory BD, et al. (2008) A link between RNA metabolism and silencing affecting *Arabidopsis* development. *Dev Cell* 14(6):854–866.
23. Hugouvieux V, Kwak JM, Schroeder JI (2001) An mRNA cap binding protein, ABH1, modulates early abscisic acid signal transduction in *Arabidopsis*. *Cell* 106(4):477–487.
24. Prigge MJ, Wagner DR (2001) The arabidopsis serrate gene encodes a zinc-finger protein required for normal shoot development. *Plant Cell* 13(6):1263–1279.
25. Park W, Li J, Song R, Messing J, Chen X (2002) CARPEL FACTORY, a Dicer homolog, and HEN1, a novel protein, act in microRNA metabolism in *Arabidopsis thaliana*. *Curr Biol* 12(17):1484–1495.
26. Boutet S, et al. (2003) Arabidopsis HEN1: A genetic link between endogenous miRNA controlling development and siRNA controlling transgene silencing and virus resistance. *Curr Biol* 13(10):843–848.
27. Papp I, Mur LA, Dalmadi A, Dulai S, Koncz C (2004) A mutation in the Cap Binding Protein 20 gene confers drought tolerance to *Arabidopsis*. *Plant Mol Biol* 55(5): 679–686.
28. Vaucheret H, Vazquez F, Crété P, Bartel DP (2004) The action of ARGONAUTE1 in the miRNA pathway and its regulation by the miRNA pathway are crucial for plant development. *Genes Dev* 18(10):1187–1197.
29. Vazquez F, Gasciolli V, Crété P, Vaucheret H (2004) The nuclear dsRNA binding protein HYL1 is required for microRNA accumulation and plant development, but not post-transcriptional transgene silencing. *Curr Biol* 14(4):346–351.
30. Lobbes D, Rallapalli G, Schmidt DD, Martin C, Clarke J (2006) SERRATE: A new player on the plant microRNA scene. *EMBO Rep* 7(10):1052–1058.
31. Yang L, Liu Z, Lu F, Dong A, Huang H (2006) SERRATE is a novel nuclear regulator in primary microRNA processing in *Arabidopsis*. *Plant J* 47(6):841–850.
32. Ishitani M, Xiong L, Stevenson B, Zhu JK (1997) Genetic analysis of osmotic and cold stress signal transduction in *Arabidopsis*: Interactions and convergence of abscisic acid-dependent and abscisic acid-independent pathways. *Plant Cell* 9(11):1935–1949.
33. Lee BH, Kapoor A, Zhu J, Zhu JK (2006) STABILIZED1, a stress-upregulated nuclear protein, is required for pre-mRNA splicing, mRNA turnover, and stress tolerance in *Arabidopsis*. *Plant Cell* 18(7):1736–1749.
34. Ishitani M, Xiong L, Lee H, Stevenson B, Zhu JK (1998) HOS1, a genetic locus involved in cold-responsive gene expression in arabidopsis. *Plant Cell* 10(7):1151–1161.
35. Kim S, et al. (2008) Two cap-binding proteins CBP20 and CBP80 are involved in processing primary MicroRNAs. *Plant Cell Physiol* 49(11):1634–1644.
36. Laubinger S, et al. (2010) Global effects of the small RNA biogenesis machinery on the *Arabidopsis thaliana* transcriptome. *Proc Natl Acad Sci USA* 107(41):17466–17473.
37. Chung T, Wang D, Kim CS, Yadegari R, Larkins BA (2009) Plant SMU-1 and SMU-2 homologues regulate pre-mRNA splicing and multiple aspects of development. *Plant Physiol* 151(3):1498–1512.
38. Fang Y, Spector DL (2007) Identification of nuclear dicing bodies containing proteins for microRNA biogenesis in living *Arabidopsis* plants. *Curr Biol* 17(9):818–823.
39. Fujioka Y, Utsumi M, Ohba Y, Watanabe Y (2007) Location of a possible miRNA processing site in SmD3/SmB nuclear bodies in *Arabidopsis*. *Plant Cell Physiol* 48(9): 1243–1253.
40. Song L, Han MH, Lesicka J, Fedoroff N (2007) Arabidopsis primary microRNA processing proteins HYL1 and DCL1 define a nuclear body distinct from the Cajal body. *Proc Natl Acad Sci USA* 104(13):5437–5442.
41. Lu C, Fedoroff N (2000) A mutation in the *Arabidopsis HYL1* gene encoding a dsRNA binding protein affects responses to abscisic acid, auxin, and cytokinin. *Plant Cell* 12 (12):2351–2366.
42. Han MH, Goud S, Song L, Fedoroff N (2004) The *Arabidopsis* double-stranded RNA-binding protein HYL1 plays a role in microRNA-mediated gene regulation. *Proc Natl Acad Sci USA* 101(4):1093–1098.
43. Sunkar R, Zhu JK (2004) Novel and stress-regulated microRNAs and other small RNAs from Arabidopsis. *Plant Cell* 16(8):2001–2019.
44. Phillips JR, Dalmay T, Bartels D (2007) The role of small RNAs in abiotic stress. *FEBS Lett* 581(19):3592–3597.
45. Sunkar R, Kapoor A, Zhu JK (2006) Posttranscriptional induction of two Cu/Zn superoxide dismutase genes in *Arabidopsis* is mediated by downregulation of miR398 and important for oxidative stress tolerance. *Plant Cell* 18(8):2051–2065.
46. Liu HH, Tian X, Li YJ, Wu CA, Zheng CC (2008) Microarray-based analysis of stress-regulated microRNAs in *Arabidopsis thaliana*. *RNA* 14(5):836–843.
47. Danin-Kreiselman M, Lee CY, Chanfreau G (2003) RNAse III-mediated degradation of unspliced pre-mRNAs and lariat introns. *Mol Cell* 11(5):1279–1289.
48. Germain A, et al. (2011) Mutational analysis of *Arabidopsis* chloroplast polynucleotide phosphorylase reveals roles for both RNase PH core domains in polyadenylation, RNA 3′-end maturation and intron degradation. *Plant J* 67(3):381–394.
49. Chen D, et al. (2011) Plant siRNAs from introns mediate DNA methylation of host genes. *RNA* 17(6):1012–1024.
50. Chinnusamy V, Stevenson B, Lee BH, Zhu JK (2002) Screening for gene regulation mutants by bioluminescence imaging. *Sci STKE* 2002(140):pl10.
51. Zheng X, Zhu J, Kapoor A, Zhu JK (2007) Role of *Arabidopsis* AGO6 in siRNA accumulation, DNA methylation and transcriptional gene silencing. *EMBO J* 26(6): 1691–1701.
52. Earley KW, et al. (2006) Gateway-compatible vectors for plant functional genomics and proteomics. *Plant J* 45(4):616–629.
53. Nakagawa T, et al. (2007) Improved Gateway binary vectors: High-performance vectors for creation of fusion constructs in transgenic analysis of plants. *Biosci Biotechnol Biochem* 71(8):2095–2100.
54. Pontes O, et al. (2006) The *Arabidopsis* chromatin-modifying nuclear siRNA pathway involves a nucleolar RNA processing center. *Cell* 126(1):79–92.

Supporting Information

Zhan et al. 10.1073/pnas.1216199109

SI Materials and Methods

Map-Based Cloning and Complementation Analysis. To clone *SIC*, map-based cloning was carried out using genomic DNA extracted from 837 F_2 plants with *sic-1* phenotype. The mutation was mapped between T22A6 and F22K18 BAC clones. All of the genes in this region were sequenced, and a mutation was found in the At4g24500 gene. *sic-2* (SALK_054171) T-DNA insertion mutant line was obtained from a publically available library collection (Arabidopsis Biological Resource Center).

For complementation assay, the At4g24500 gene, including 2,112 bp upstream of the initiation codon and 529 bp downstream of the stop codon, was PCR amplified by LA Taq polymerase (Takara) using WT genomic DNA as template. The resulting 4,123-bp fragment was cloned into the pCR2.1 TOPO vector (Invitrogen) and then subcloned into pCAMBIA1200 between the SacI and BamHI sites. This and all other constructs described here were completely sequenced to ensure that they did not contain PCR or cloning errors. The binary construct was then introduced into *Agrobacterium* strain GV3101 and was used for genetic transformation of the *sic-1* plants by the floral dip method. Hygromycin-resistant transgenic plants were selected to check complementation.

Nuclear Run-On Analysis. Nuclei isolation and in vitro transcription reactions were performed using 2-wk-old seedlings as described previously (1). Equal amounts of labeled RNA for treated and untreated samples of WT and *sic-1* seedlings were used for filter hybridization. Nuclear run-on analysis and quantification of transcription rates were performed as described previously (2).

Tiling Array Analysis. Total RNA was extracted from 10-d-old seedlings and treated with DNase (Qiagen), and RNA integrity was determined on a Bioanalyzer. Whole-transcript targets for tiling array hybridization were prepared by using the GeneChip Whole Transcript Double-Stranded cDNA Synthesis Kit and the GeneChip Whole Transcript Double-Stranded DNA Terminal Labeling Kit (Affymetrix). Targets were hybridized to GeneChip *Arabidopsis* Tiling 1.0R Array (Affymetrix) in duplicate.

Tiling array probes were first remapped to the *Arabidopsis* genome (TAIR9) using SOAP2 (3), and only probes that perfectly matched to a unique position in the genome were used for subsequent analyses. A custom Chip Definition File was created using the mapping result and was used to quantile-normalize raw tiling array data with the aroma.affymetrix framework (4). To identify genes that were differentially expressed in the mutant vs. the WT, we first used the genefilter package in Bioconductor (http://www.bioconductor.org/) to remove genes that showed low expression level (normalized signal intensity was <100 in all libraries) and genes that showed little change in gene expression across samples (interquartile range of log2-intensities was <0.5). We then applied the linear model method implemented in the limma package in Bioconductor to identify genes that showed differential expression. The "BH" method (5) was used to adjust for multiple comparisons.

For the analysis of intron retention, we first calculated the log2-signal intensity for each annotated intron (TAIR9) according to the trimmed-mean of signal intensities from all mapped probes. Introns with fewer than three mapped probes or low expression (expression was <32 in all samples) were removed from further consideration. We then used the SAM algorithm (6) to identify introns that showed significantly higher expression in the mutant than in the WT. A false discovery rate of 0.05 was used as the significance cutoff.

1. Dorweiler JE, et al. (2000) mediator of paramutation1 is required for establishment and maintenance of paramutation at multiple maize loci. *Plant Cell* 12(11):2101–2118.
2. Lee BH, Kapoor A, Zhu J, Zhu JK (2006) STABILIZED1, a stress-upregulated nuclear protein, is required for pre-mRNA splicing, mRNA turnover, and stress tolerance in *Arabidopsis*. *Plant Cell* 18(7):1736–1749.
3. Li R, et al. (2009) SOAP2: An improved ultrafast tool for short read alignment. *Bioinformatics* 25(15):1966–1967.
4. Bengtsson H, Simpson K, Bullard J, Hansen K (2008) *Aroma.affymetrix: A Generic Framework in R for Analyzing Small to Very Large Affymetrix Data Sets in Bounded Memory* (Univ of California, Berkeley).
5. Benjamini Y, Hochberg Y (1995) Controlling the false discovery rate—a practical and powerful approach to multiple testing. *J R Stat Soc B* 57:289–300.
6. Tusher VG, Tibshirani R, Chu G (2001) Significance analysis of microarrays applied to the ionizing radiation response. *Proc Natl Acad Sci USA* 98(9):5116–5121.

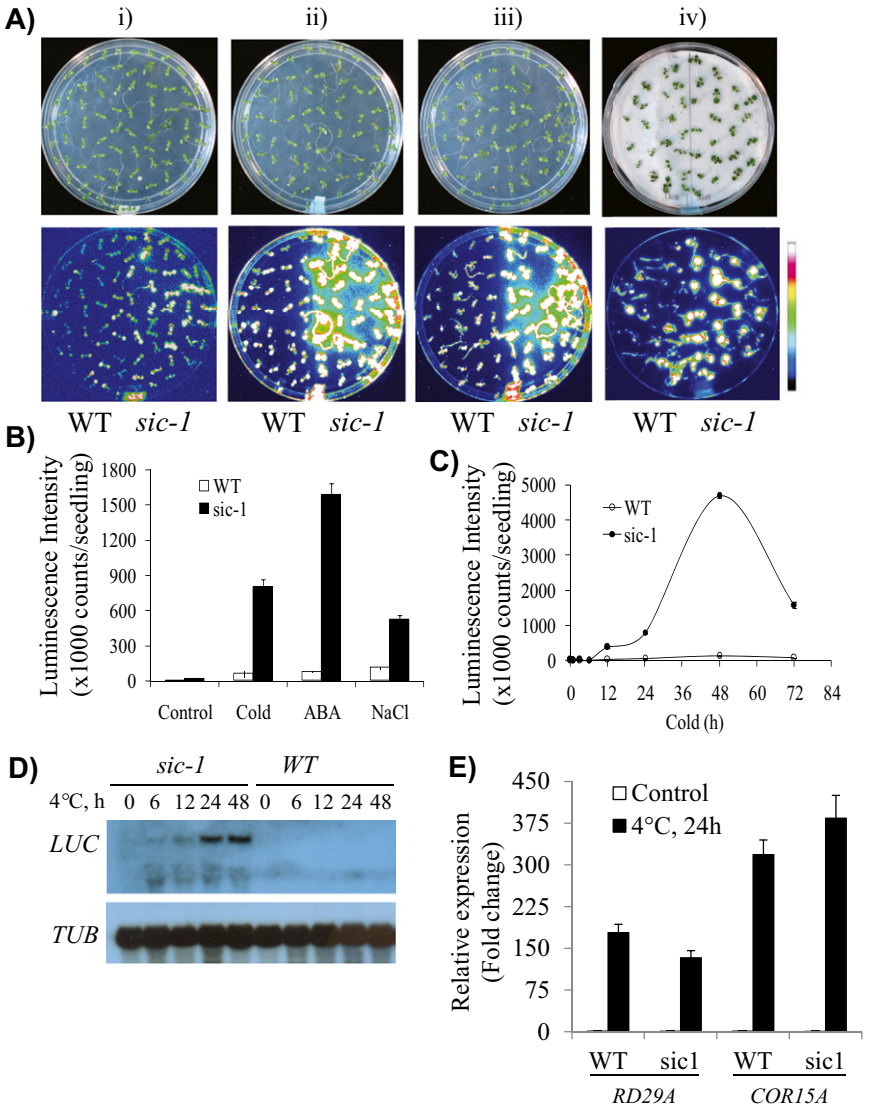

Fig. S1. *RD29A:LUC* luminescence of WT and *sic-1* seedlings after cold, salt, or abscisic acid (ABA) treatment, and stabilized *LUC* transcript in *sic-1*. (*A*) Bioluminescence image of WT and *sic-1*. (*i*) Control; (*ii*) cold, 4 °C, 24 h; (*iii*) ABA 100 μM, 3 h; (*iv*) NaCl, 150 mM, 3 h. *Upper*: Visual images; *Lower*: LUC images (LUC bioluminescence from *sic-1* was very strong, and thus *sic-1* side of the plate is brighter than the WT side). (*B*) Quantification of the luminescence of WT and *sic-1* seedlings in *A i–iv*. (*C*) Induction of *RD29A:LUC* in WT and *sic-1* after different durations of cold stress. (*D*) Northern analysis of *LUC* expression. (*E*) Quantitative RT-PCR analysis of *RD29A* and *COR15A* expression.

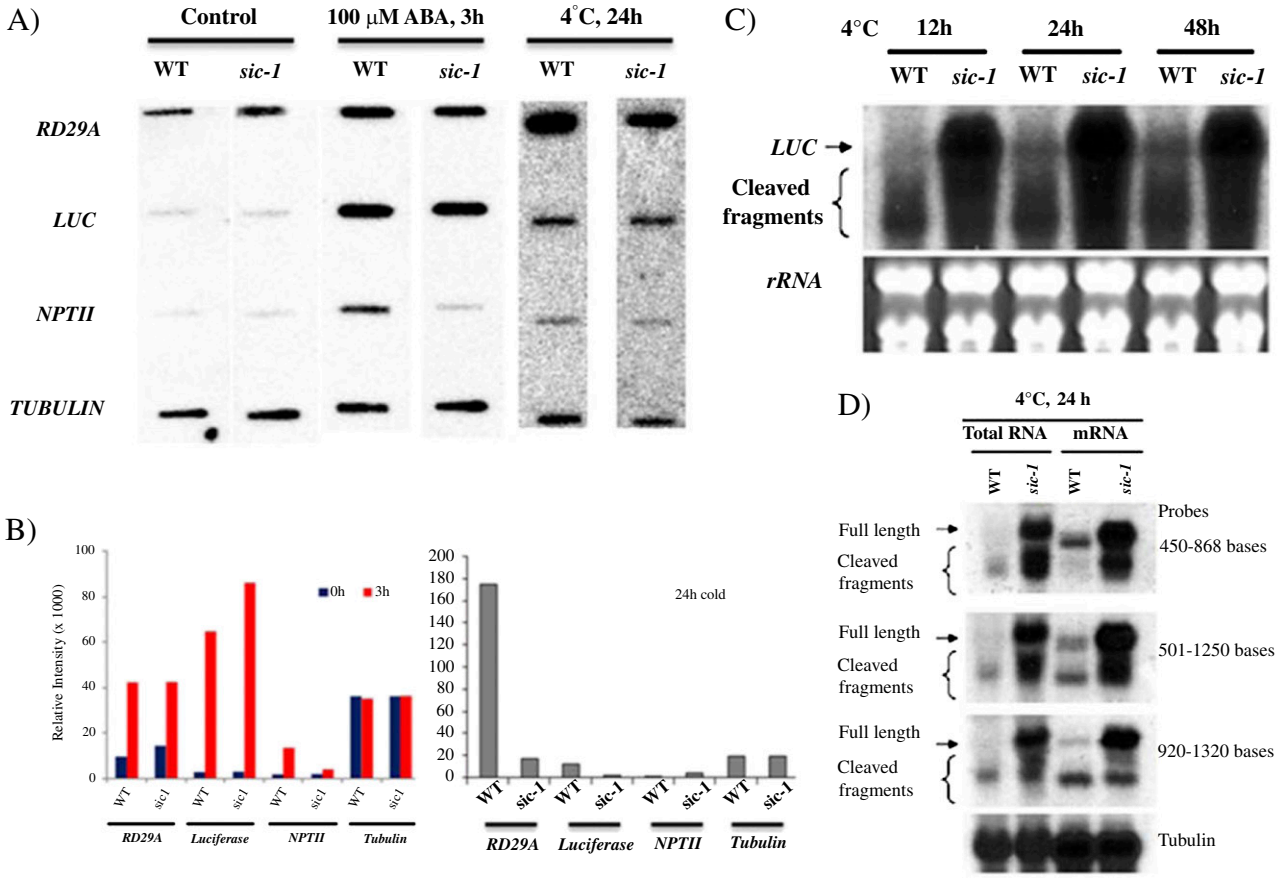

Fig. S2. Nuclear run-on analysis and Northern blot analysis of gene expression. (*A*) Nuclear run-on analysis of *RD29A* and *RD29A:LUC* in WT and *sic-1* under ABA 3 h and cold 24 h. (*B*) Relative expression of genes in nuclear run-on analysis with ABA and cold treatments (quantified of signal intensities). (*C*) Northern blot analysis of *LUC* expression during cold stress. The blot was probed with full-length *LUC* coding sequence probe. (*D*) Northern blot analysis of *LUC* expression at 0 and 24 h after cold stress. The blots were probed with 450–868, 501–1,250, or 920–1,320 base fragment of *LUC* coding sequence.

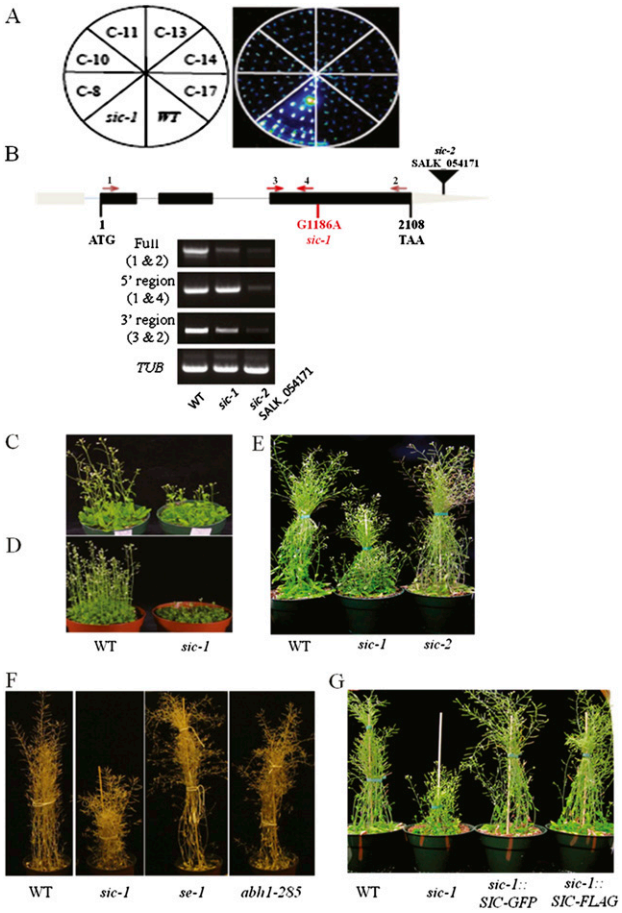

Fig. S3. Complementation assay and *sic-1* developmental defect. (*A*) Molecular complementation of *SIC*. *SIC* gene (with its native promoter, coding sequence (CDS), and terminator) was cloned from WT and transformed into *sic-1*. Bioluminescence image of T1 transgenic (*sic*:*SIC*) seedlings (C-8, 10, 11, 13, 14, and 17), *sic-1*, and WT seedlings after 24 h of cold stress. (*B*) RT-PCR analysis of *SIC* gene in WT, *sic-1*, and *sic-2*. (*C*) Plants grown under long-day (16 h light) conditions. (*D*) Plants grown under short-day (8 h light) conditions. (*E*) *sic-1 and sic-2* under long-day conditions at maturity. (*F*) Comparison of plant height in *sic-1*, *se-1*, and *abh1-285*. (*G*) Restoration of plant height in *sic-1* complemented lines.

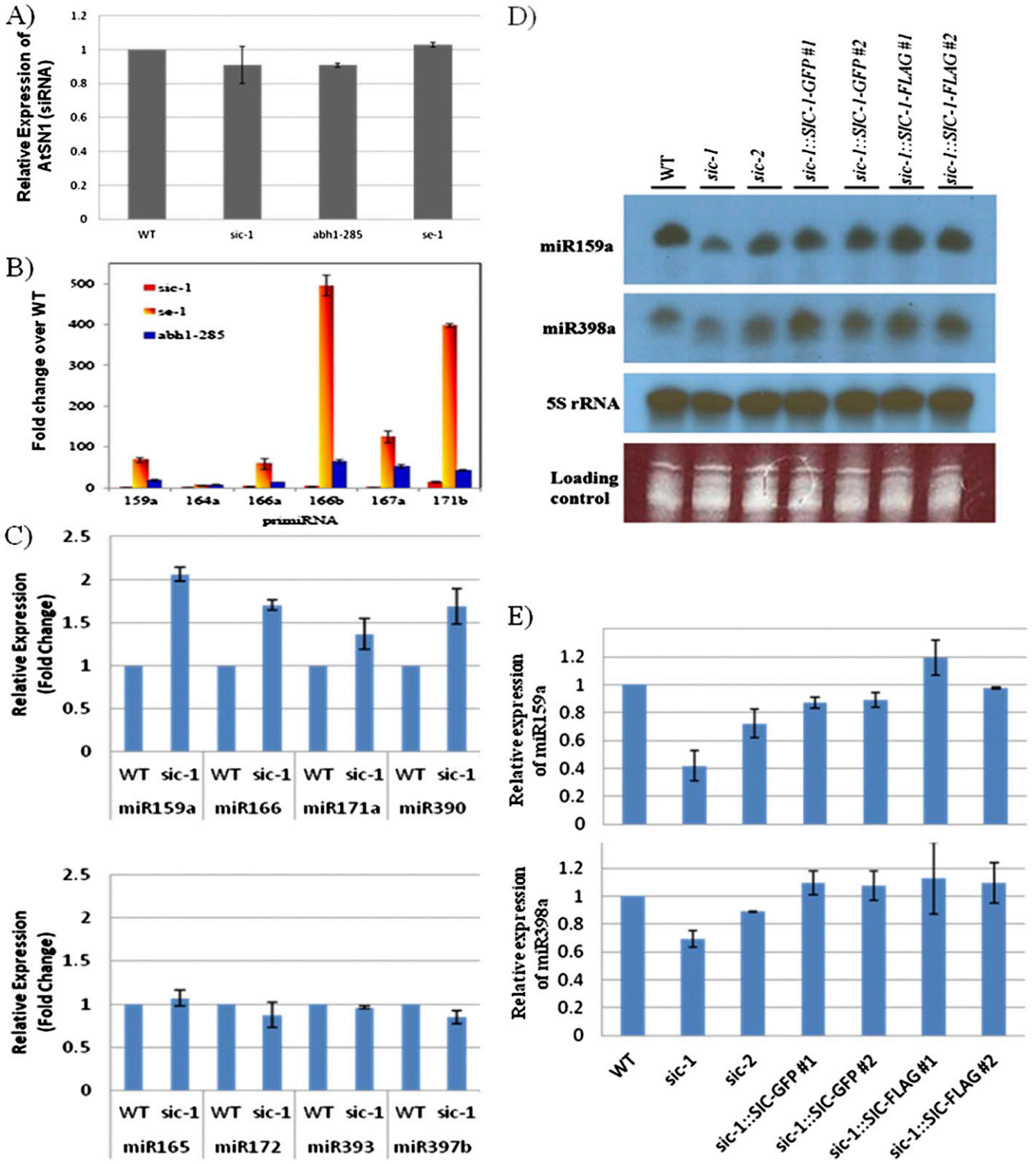

Fig. S4. Accumulation of miRNAs, pri-miRNAs, and miRNA target genes. (*A*) Taqman RT-PCR analysis of *AtSN1* (siRNA) level in WT, sic-1, abh1-285, and se-1. (*B*) Quantitative RT-PCR analysis of pri-miRNA accumulation in WT, *sic-1*, *se-1*, and *abh1-285*. (*C*) Quantitative RT-PCR analysis of miRNA target genes in WT and *sic-1*. *Upper*: Increase in expression of some predicted miRNA targets; *Lower*: no change in expression of some predicted miRNA targets. (*D*) Northern blot analysis of accumulation of miR159a and miR398a levels in WT, *sic-1*, *sic-2*, *sic-1:SIC-GFP #1*, *#2*, *sic-1:SIC-FLAG #1*, and *#2*. (*E*) Taqman RT-PCR analysis of miR159a and miR398a levels in WT, *sic-1*, *sic-2*, *sic-1:SIC-GFP #1*, *#2*, *sic-1:SIC-FLAG #1*, and *#2*.

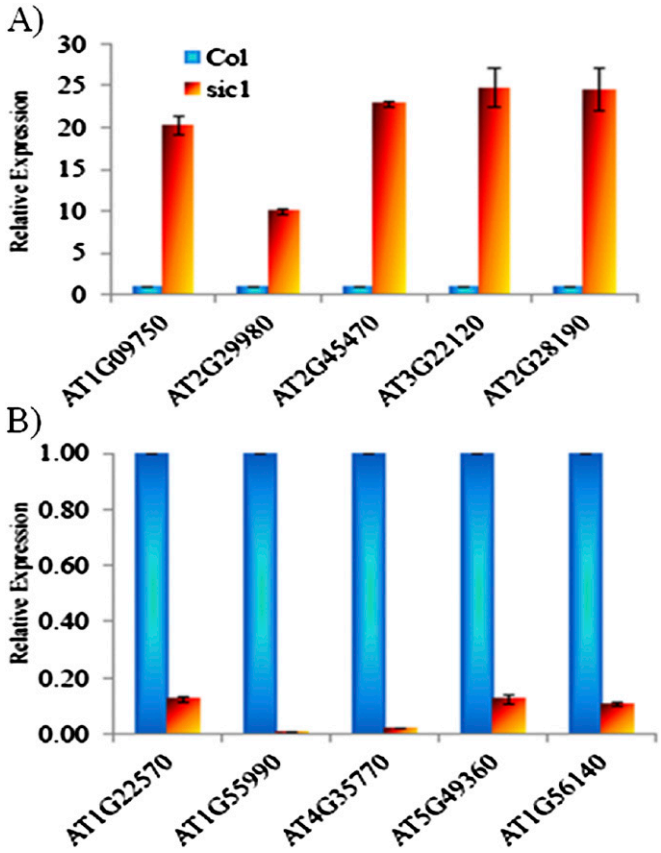

Fig. S5. Validation of tiling array gene expression data by quantitative RT-PCR analysis. (*A*) Up-regulated genes; (*B*) down-regulated genes. Gene expression level in the *sic-1* mutant is presented as a fold change relative to that in WT plants under 4 °C cold stress for 24 h.

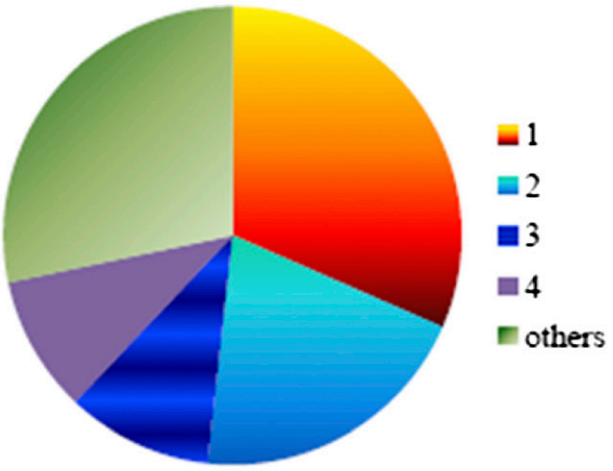

Intron position

No. of introns		%
1	144	31.6
2	92	20.2
3	47	10.3
4	44	9.6
others	129	28.3

Fig. S6. Distribution of intron positions in genes with impaired intron splicing in the *sic-1* mutant.

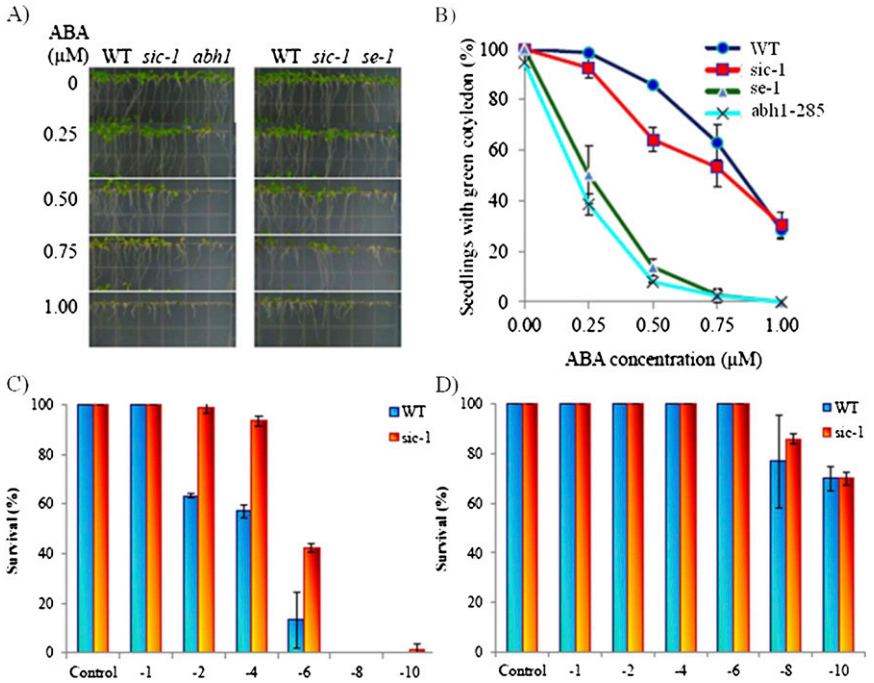

Fig. S7. ABA sensitivity and freezing tolerance of *sic-1*. (*A*) Germination and seedling growth of WT, *sic-1*, *se-1*, and *abh1-285* on MS supplemented with 0.0, 0.25, 0.50, 0.75, or 1.0 μM ABA. (*B*) Percentage of seedlings with green cotyledons when grown on MS medium supplemented with 0.0, 0.25, 0.50, 0.75, or 1.0 μM ABA. (*C*) Freezing tolerance of WT and the *sic-1* seedlings without cold acclimation. (*D*) Freezing tolerance of WT and the *sic-1* seedlings after cold acclimation.

Table S1. List of oligonucleotides used in this study.

Purpose	Name	Sequence
Genetic complementation	SIC1c-Forward	CGGGATCCGTGCGTTGAAGTTATATCCTCTG
	SIC1c-Reverse	GAGCTCCATTAGAGTTGGACAGTTGAGTCATC
FLAG-, HA3x-GFP-tag	SIC1-TAG-Forward	CACCGTGCGTTGAAGTTATATCCTCTG
	SIC1-TAG-Reverse	ATTGCTTGACTCATCGCATGTAGCA
Amplification of Northern probe	CRB-exon-Forward	GTGGAGAAAGCAAAGCATGTCCTC
	CRB-exon-Reverse	GTTTCTTCATCGTCCCTAGCTTGAC
	CRB-intron-Forward	GTTCTGCTTTTGTGTGTCTGATGAG
	CRB-intron-Reverse	GACTAGTGATAGAATCTGAAGGCA
	CAX1-exon-Forward	CTGACTGACGCCACAATAGGTG
	CAX1-exon-Reverse	TCGTGACAGAGCCGTGGTCAGTAG
	CAX1-intron-Forward	GTTTGTACTATGCTGTCACGTTGAC
	CAX1-intron-Reverse	AGAGTAAGTATCCGACCATCATC
Quantitative RT-PCR for validation of tiling array data	AT1G09750-Forward	GACCCAGTGTATTTGACGTTTGAC
	AT1G09750-Reverse	AGAATGACGACACATTCACCTGCT
	AT2G29980-Forward	CAATGAGTTACGTCGTCAGAGAC
	AT2G29980-Reverse	GTAGAGGAATGTCTGAGAAACTC
	AT2G45470-Forward	CACGACGATTACAGTTCTCGTC
	AT2G45470-Reverse	GTGCCTTTGGAGATCTTGTGGAG
	AT3G22120-Forward	AGGTTTACTTGACCTAGACGCAG
	AT3G22120-Reverse	CAGAGACTCTCAACGTTCTACATC
	AT2G28190-Forward	GAAGAGCCTTTGTGGTTCACGAG
	AT2G28190-Reverse	AAGAGTACTTGCTTAGCCTCTGAC
	AT1G22570-Forward	TCGTGCTCACCACGTATGTGATC
	AT1G22570-Reverse	CTATTGGAGGATGGTCAGTCCGAG
	AT1G55990-Forward	CAATGATGATCAACACTTGCTCAG
	AT1G55990-Reverse	CTGATGGCATTGGAAATGGAGAC
	AT4G35770-Forward	GATCTTCTCACTGCTGGCTTCAC
	AT4G35770-Reverse	TACTTGCGTTGAGAACATCTACAG
	AT5G49360-Forward	CACCAATGTGCAGCTTATGCTCAC
	AT5G49360-Reverse	CGTTCGAGAAGGTTCATGTCATG
	AT1G56140-Forward	GTGGTGTCATCAAATCTCCAGTC
	AT1G56140-Reverse	CACAAACATCTCATGCCTTGAGAC
Probes for miRNA Northern blot analysis	miR157a	GTGCTCTCTATCTTCTGTCAA
	miR159a	TAGAGCTCCCTTCAATCCAAA
	miR164a/b	TGCACGTGCCCTGCTTCTCCA
	miR165	GGGGGATGAAGCCTGGTCCGA
	miR166a-g	GGGGAATGAAGCCTGGTCCGA
	miR168a/b	TTCCCGAGCTGCACCAAGCGA
	miR171a	GATATTGGCGCGGCTCAATCA
	miR172a/b	ATGCAGCATCATCAAGATTCT
	miR173a	GTGATTTCTCTCTGCAAGCGAA
	miR393a/b	GATCAATGCGATCCCTTTGGA
	miR398a	AAGGGGTGACCTGAGAACACA
	miR414	TGACGATGATGATGAAGATGA
	ta-siR255	TACGCTATGTTGGACTTAGAA
	ta-siR752	AACGCTATGTTGGACTTAGGA
	ta-siR850	GTCGATATGTTGAACTTAGAA
pri-miRNA	pri-miR156a-F	ATTGTTCACTCTCAAATCTCAAG
	pri-miR156a-R	AAGAGATCAGCACCGGAATCTG
	pri-miR164a-F	CATACTACAAACGCCCCTCATG
	pri-miR164a-R	ACTAACATTATTGTAAAACCAG
	pri-miR164a-R (Intron spanning)	ATGCGTTACATATGCCTTTTAG
	miR159a-qF	GGTCTTTACAGTTTGCTTATG
	miR159a-qR	AGAAGGTGAAAGAAGATGTAG
	miR166a-qF	cccgggATCACCACTCACTTATCTTCTTC
	miR166a-qR	cccgggTAATTTGAAAAGAAGGAAGAAATATG
	miR166b-qF	cccgggATCATTCTCTTCATCATCACCAC
	miR166b-qR	cccgggATGGACAAATCTTCTTCGTTAATTCG
	miR171b-qF	CTCTAAGGCTACCGATCGAGTG
	miR171b-qR	CTCCAGGATCCGATGGTTCTCTC
	TBQ10-qF	GGCCTTGTATAATCCCTGATGAATAAG
	TBQ10-qR	AAAGAGATAACAGGAACGGAAACATAGT

Table S1. Cont.

Purpose	Name	Sequence
Taqman quantitative PT-PCR for miRNA	Taqman miR159a	TTTGGATTGAAGGGAGCTCTA
	Taqman miR398a	TGTGTTCTCAGGTCACCCCTT
Quantitative RT-PCR for *COR* genes	RD29A-qForward	CTTGATGGTCAACGGAAGGT
	RD29A-qReverse	CAATCTCCGGTACTCCTCCA
	COR15A-qForward	GCTTCAGATTTCGTGACGGATAAAAC
	COR15A-qReverse	GCAAAACATTAAAGAATGTGACGGTG
	Actin2-qForward	TAACAGGGAGAAGATGACTCAGATCA
	Actin2-qReverse	AAGATCAAGACGAAGGATAGCATGAG

Other Supporting Information Files

Dataset S1 (XLSX)
Dataset S2 (XLSX)
Dataset S3 (XLSX)